

Instrument Calorimeter-II- The microcalorimeters

Flavio Gatti

University and INFN of Genoa

Few historical notes

- The first calorimetric experiment was applied to the beta decay and has been made by Ellis and Wooster in 1927
 - At that time it was the problem of understanding why “ β -ray” were continuous spectra instead of “ α -ray” that were emitted as mono-energetic lines by nuclei, as expected within the general framework of the quantum theory of the “disintegration of the bodies”
-

The Average Energy of Disintegration of Radium E.

By C. D. ELLIS, Ph.D., Lecturer in the University of Cambridge, and W. A. WOOSTER, B.A., Charles Abercrombie Smith Student of Peterhouse, Cambridge.

(Communicated by Sir Ernest Rutherford, O.M., F.R.S.—Received August 3, 1927.)

After several trials the calorimeter which was finally used consisted of two lead tubes, 13 mm. long and 3.5 mm. diameter, each with a central hole of rather more than 1 mm. diameter. Each calorimeter fitted exactly into a thin outer sheath of silver, and were supported as shown in fig. 2 (a) by two discs of mica A and B, which in turn were carried by the brass screw C fitting into an ebonite base DE. The thermocouples were insulated by the thinnest mica possible, a sheet of the latter being attached to the calorimeter tubes by a very small quantity of soft wax. The thermocouples were laid on this sheet of mica with a little wax at the junctions, and then another piece of mica laid on top and the whole pressed together with a hot iron.* The two lead calorimeters were made as nearly alike as possible so as to minimise the effect of external variations of temperature on the difference of temperature between them. In order still further to reduce these externally induced temperature differences, the whole calorimeter system was placed in a small cavity in a copper block, as

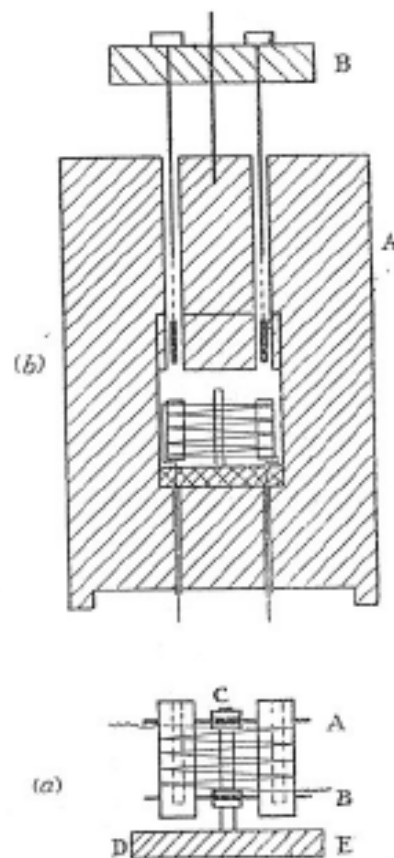


FIG. 2.

Interesting follow-up

- “ β -spectrum is continuum because of the slowing down in the material” (Lisa Meitner) or “in collision with atomic electron” (E.Rutherford)
 - → “Not conservation of energy” (N.Bohr)
 - The results was $\langle E \rangle_{\text{calorimeter}} = 0.33 \pm 0.03$ MeV/atom against $E_{\text{max}} = 1.05$ MeV/atom
 - → $E_{\text{max}} - \langle E \rangle$ “carried out by escaping particle”
 - Pauli conjecture of the neutrino (1930)
 - First fully calorimetric detector of heat produced by particles, even if not able to detect single particle.
-

Cryogenic calorimeter

- ❑ Once the LHe and the superconductivity was discovered, several ideas on thermal detection of single particles were proposed and tested.
 - ❑ Big calorimeters were used at low temperature for studying fundamental properties of materials
 - ❑ But in 1941, D.H. Andrews suggested first and executed in 1949 an experiment that anticipated the present most developed and advanced technology of microcalorimeters.
-

Single particle detection with thermal detector in 1949: a technique incredibly similar to the present one

The Effect of Alpha-particles on a Superconductor*

D. H. ANDREWS, R. J. DE SORBO,
Chemistry Department, The Johns Hopkins University

SUPERCONDUCTING bolometers have been used for the detection of alpha-particles from a source through a countable electrical pulse produced by the impact. The bolometer used was made of a strip of columbite, 0.006 mm, mounted within a cryostat, as previously described, and maintained at the center of the transition, half-way between superconductivity; it was relatively constant over a 0.04° wide and fell sharply both above and below the transition zone, being reduced approximately to noise level on a decrease or increase of 0.1°K . The electrical resistance was 2ω in the normal state at 15°K .

The source consisted of a thin mica window, and the air pressure in the chamber was at 0.01 mm. The number of counts per second was also a function of the energy of the alpha-particles passing through the CbN, being at a maximum for a certain energy.

The source was placed at a distance of 2 cm to 20 cm from the center of the transition, half-way between superconductivity; it was relatively constant over a 0.04° wide and fell sharply both above and below the transition zone, being reduced approximately to noise level on a decrease or increase of 0.1°K . The electrical resistance was 2ω in the normal state at 15°K .

The number of counts per second was also a function of the energy of the alpha-particles passing through the CbN, being at a maximum for a certain energy. The number of counts per second was also a function of the energy of the alpha-particles passing through the CbN, being at a maximum for a certain energy.

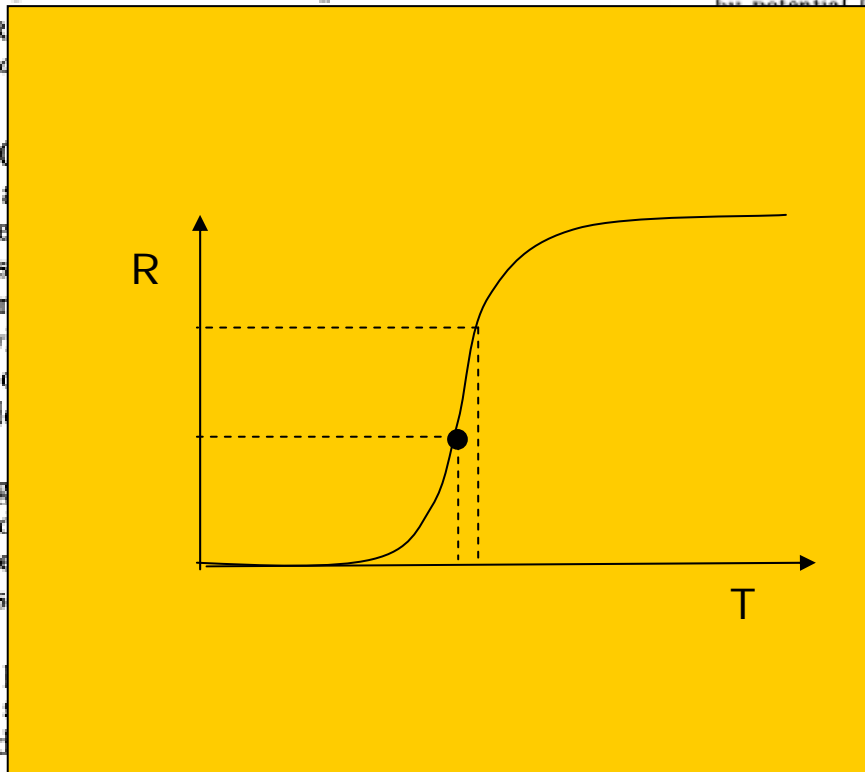


TABLE I. Comparison of α -particle counts with ionization chamber and bolometer.

Distance from source to defining area:	20 cm	2 cm
Average counts per second:		
(a) Ionization chamber	40	740
(b) Bolometer	32	660

of energy. The bolometer was protected from general heat radiation by a shield held at 90°K . The α -particles passed through a hole in this shield, the opening being 7 mm diameter, in alignment with the bolometer.

The bolometer was connected to a direct current supply, and the potential leads to the primary of an audio transformer, the secondary of which led to a pulse amplifier, and thence to an audio amplifier and scale-of-1000 counter.

The counting was at a maximum when the CbN was at the center of the transition, half-way between superconductivity; it was relatively constant over a 0.04° wide and fell sharply both above and below the transition zone, being reduced approximately to noise level on a decrease or increase of 0.1°K . The electrical resistance was 2ω in the normal state at 15°K .

The number of counts per second was also a function of the energy of the alpha-particles passing through the CbN, being at a maximum for a certain energy.

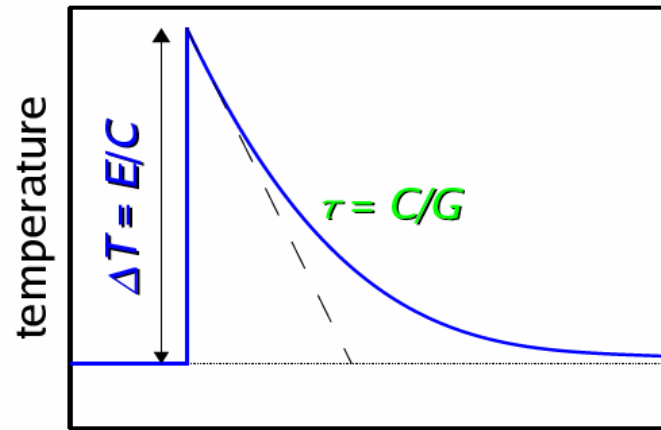
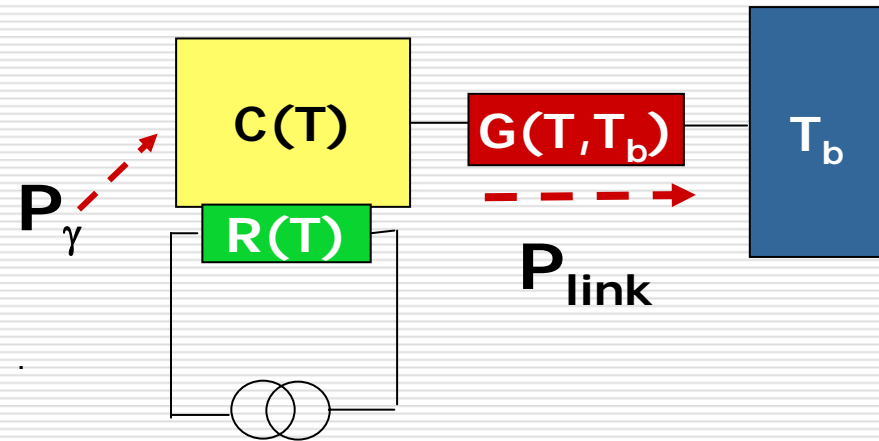
The number of alpha-particles counted with the bolometer agreed, within experimental error, with the number counted with an ionization chamber through a slit system similar in geometry to that used in the bolometer experiments. The ionization chamber slit was 0.01 mm wide, and the air pressure in the chamber was at 0.01 mm.

From the width of the peaks on the oscilloscope it is estimated that the width of an individual pulse from the bolometer is about 10^{-7} volt second wide. The maximum signal to noise ratio is about 10^3 . The pulse height may be expected to be proportional to the energy of the α -particle, experiments are being conducted to evaluate the signal to noise ratio, in order to evaluate the energy with which the energy of individual particles can be determined by this method, and to determine the kind of pulses produced when superconducting bolometers of this and other materials are exposed to different kinds of particle radiation. The authors wish to thank Professor Walter Koski and Mr. Carl Thomas for valuable advice and assistance.

This work was supported in part by contract N5-ORi-166, Task IV, ONR U. S. Navy, and in part by a grant from Dr. H. A. B. Dunning.

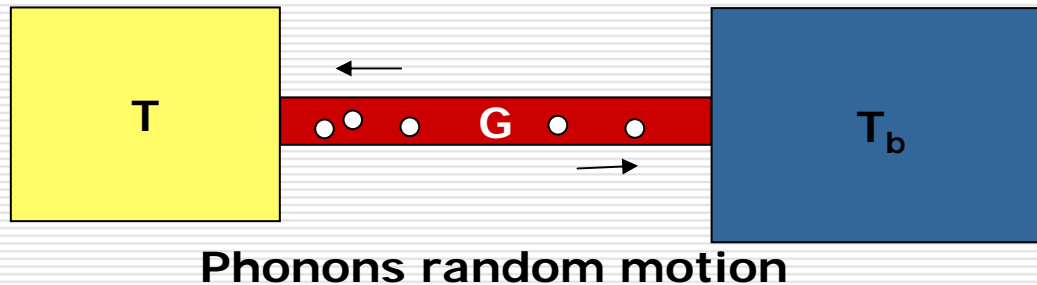
* This work was supported in part by contract N5-ORi-166, Task IV, ONR U. S. Navy, and in part by a grant from Dr. H. A. B. Dunning.
¹ Andrews, Milton, and DeSorbo, *J. Opt. Soc. Am.* **36**, 518 (1946).

What is a Microcalorimeter for spectroscopy.



- A simple model of a microcalorimeter as tool for spectroscopy is composed by:
 - Absorber of heat capacity C
 - Thermal link with conductance G
 - Thermistor $R(T)$
 - Biasing and read-out circuit
 - Thermal bath
-

Why cryogenic calorimeter are so attractive? → “incredible” intrinsic energy resolution in single quantum detection



- ❑ T rms fluctuations determined by phonon brownian motion between the two bodies
 - ❑ Average phonons $\langle N \rangle = U/kT = CT/kT$
 - ❑ Internal energy fluctuation $\Delta U_{\text{rms}} = (N)^{1/2} \times kT = (kT^2C)^{1/2}$
 - ❑ RMS Intrinsic Energy Noise $\approx (kT^2C)^{1/2}$
 - ❑ Ex: $T=0.1 \text{ K}$, $C=10^{-13} \text{ J/K} \rightarrow \Delta U_{\text{rms}} \approx 1\text{eV}$
-

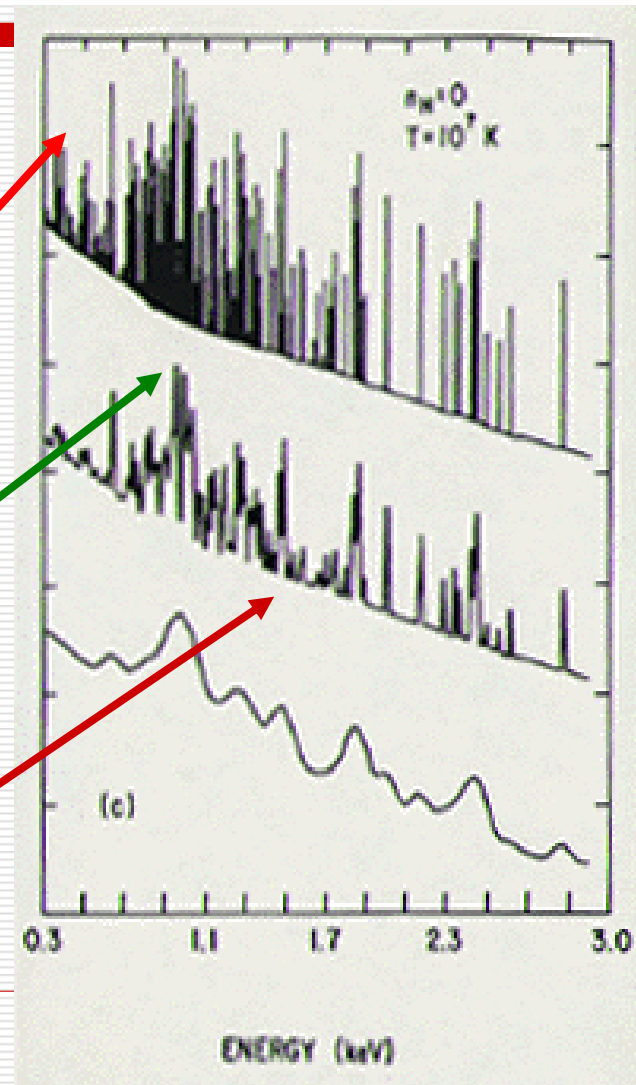
They can perform very high resolution Energy Dispersive X ray Spectroscopy (EDXRS). Ex.: hot plasma of ISM/IGM

plasma emission
(10^7K) observed with:

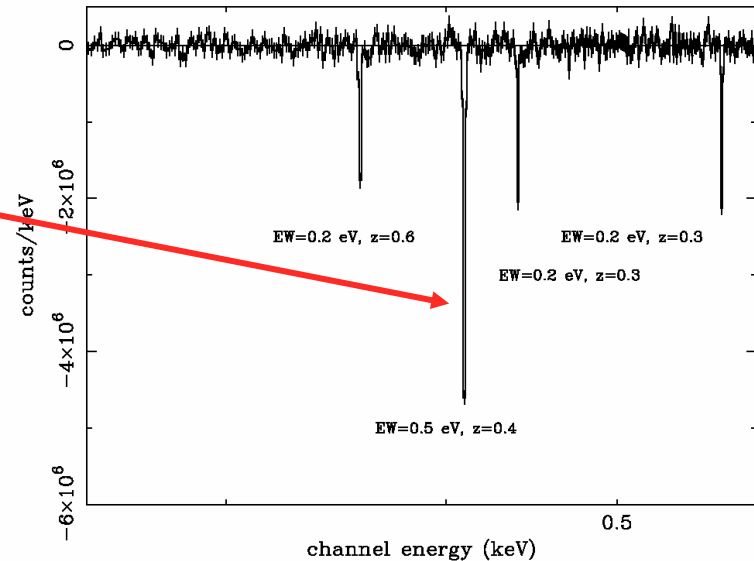
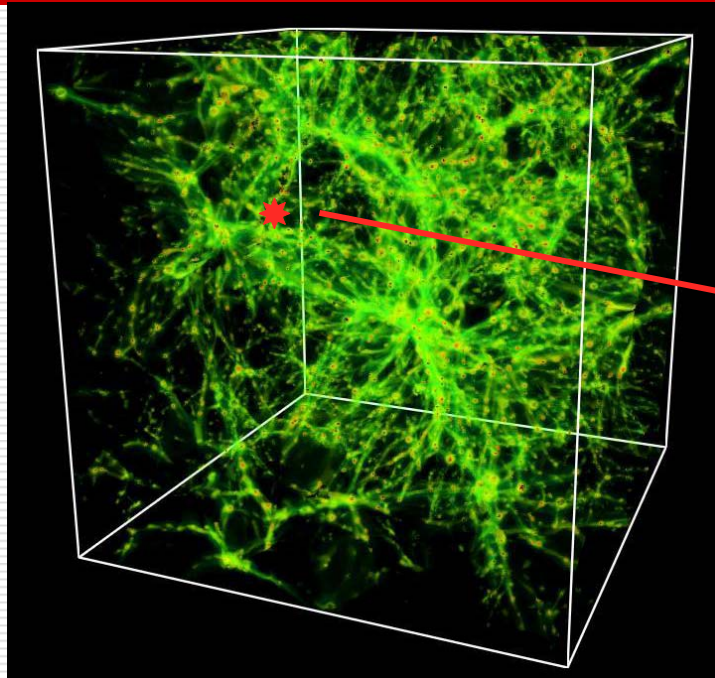
* Next generation (TES) ucal
($\Delta E=2\text{ eV}$: XEUS/Con-X)

* present generation ucal
($\Delta E=6-8\text{ eV}$: ASTRO-E (?))

* CCD ($\Delta E=100\text{ eV}$: XMM)



They can perform very high resolution Energy Dispersive X ray Spectroscopy (EDXRS). Ex: WHIM and Dark Matter

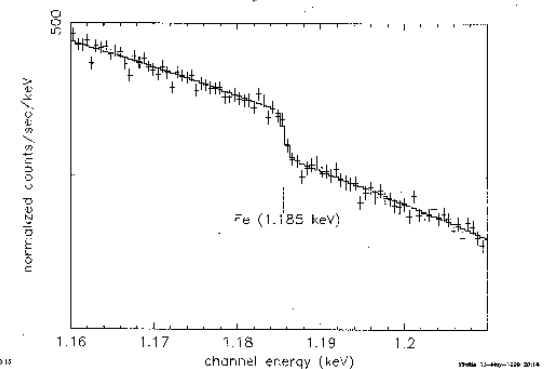
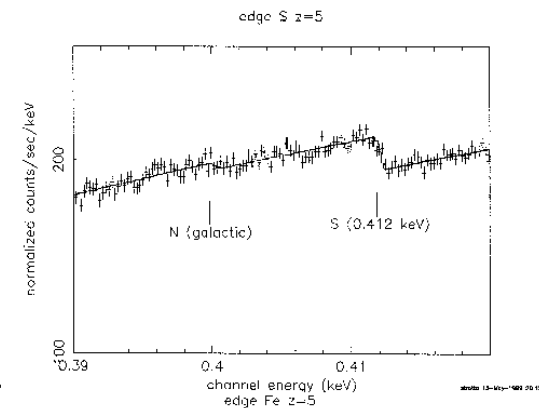
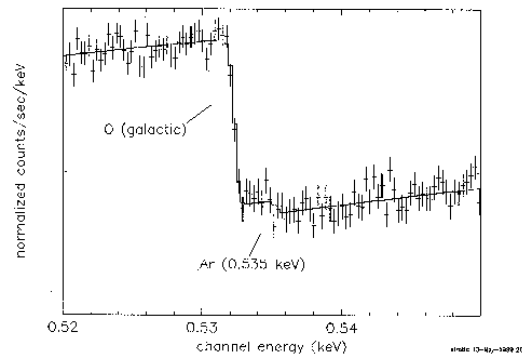
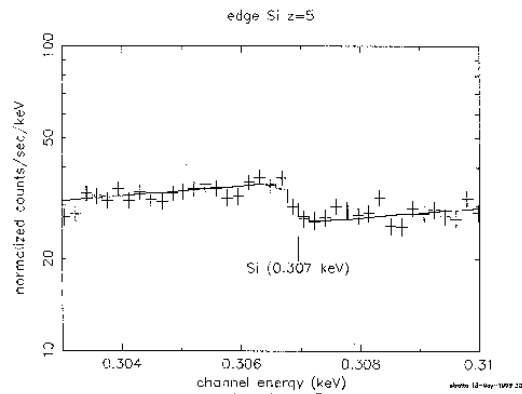
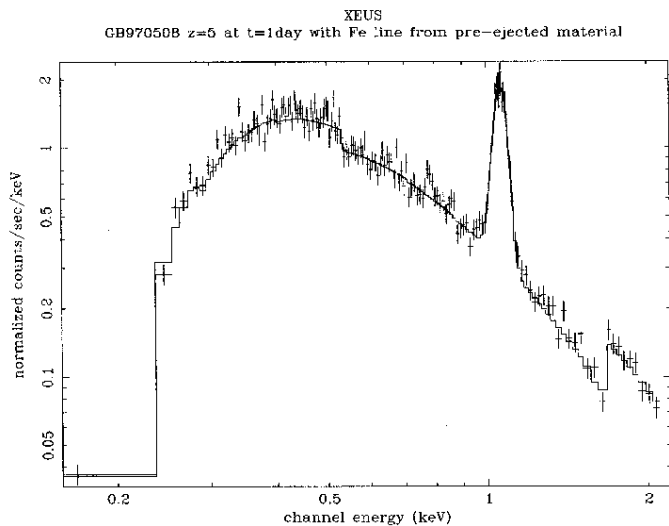


Simulations of WHIM absorption features from OVII as expected from filaments (at different z, with EW=0.2-0.5 eV) in the l.o.s. toward a GRB with Fluence = 4×10^{-6} as observed with ESTREMO (in 100 ksec). About 10% of GRB (10 events per year per 3 sr) with 4 million counts in the TES focal plane detector

Ex: study of local and intergalactic medium in primeval galaxies with GRB with XEUS-like mission

- The Fe line in a GRB like GB970508 but at $z=5$

- Study of the metallicity of the ISM of a host galaxy of a GRB at $z=5$ through X-ray edges



Microcalorimeter model

- Steady state with only Joule power

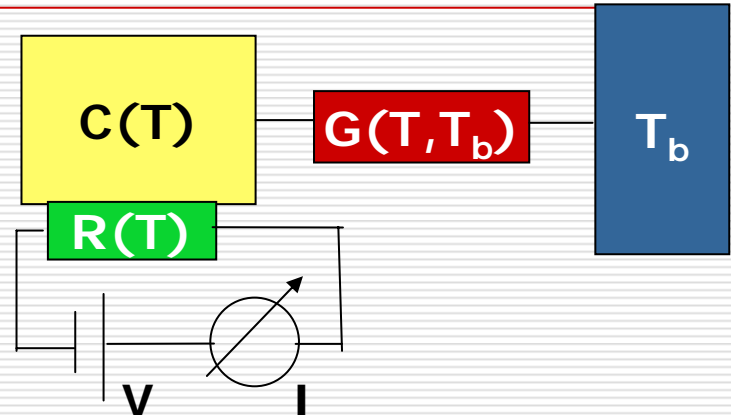
$$W(T_0, T_b) = P_{J0}$$

- Thermal evolution at impulsive

$$C \frac{dT}{dt} + W(T, T_b) = P_J(t) + P_\gamma(t)$$

- Within the limit of small signal, the difference of the two powers, $W(T, T_b)$ and $W(T_0, T_b)$, flowing in the thermal link are approximated by the thermal conductance $G \times \delta T$

$$W(T, T_b) - W(T_0, T_b) \cong \frac{dW(T, T_b)}{dT} \delta T = G \delta T$$



Microcalorimeter model

- As before, for small signals, we can approximate the differences of the two bias Joule power as follow

$$P_J(t) - P_{J_0} \cong \frac{d}{dT} \left(\frac{V^2}{R} \right) \delta T = -\frac{V_0^2}{R_0} \frac{T}{R} \frac{dR}{dT} \frac{1}{T} \delta T \cong -P_{J_0} \alpha \frac{1}{T_0} \delta T$$

in case of voltage biased microcalorimeter
(Attention → only for voltage bias)

- Where the thermometer sensitivity: $\alpha = \frac{T}{R} \frac{dR}{dT}$
-

Microcalorimeter model

- Subtracting term by term the thermal equations and making the first order approx. the simplest equation of the microcalorimeter looks as follow

$$\frac{d\delta T}{dt} = -\frac{1}{C} \left(G + \frac{P\alpha}{T} \right) \delta T + P_\gamma = -\left(\frac{C}{G} \right)^{-1} (1+L) \delta T + P_\gamma$$

- **Thermal time constant**

$$\tau = \frac{C}{G}$$

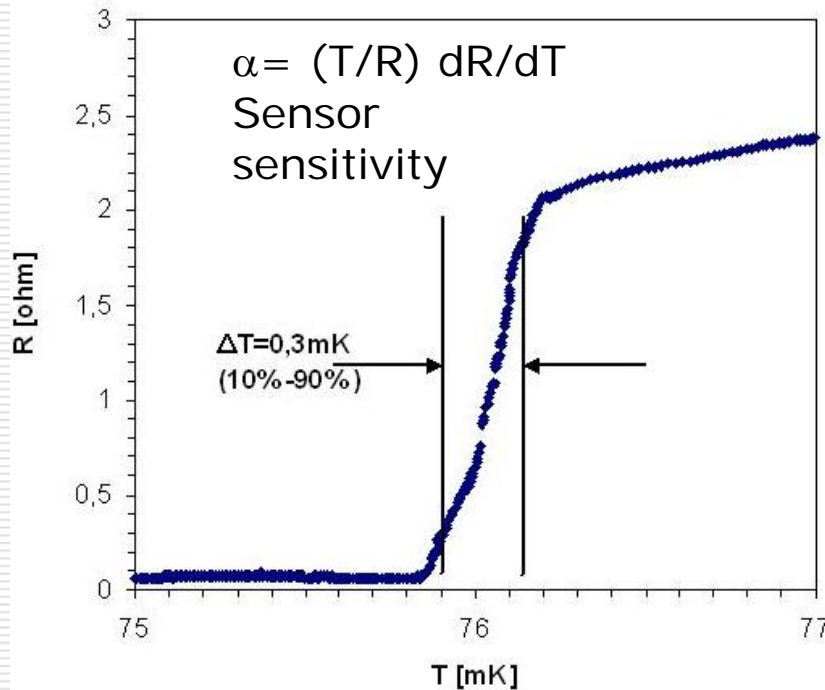
- **Electrothermal feedback parameter**

$$L = \frac{P\alpha}{GT}$$

- **ETF time constant**

$$\tau_{ETF} = \frac{\tau}{1+L}$$

An example: case of superconducting Transition Edge Sensor (TES)



- Insert Sensor Model
- Insert bias power for sensor readout
- Make the realistic model of the detector thermal/electrical components
- Make a realistic model of all the power flow mechanism

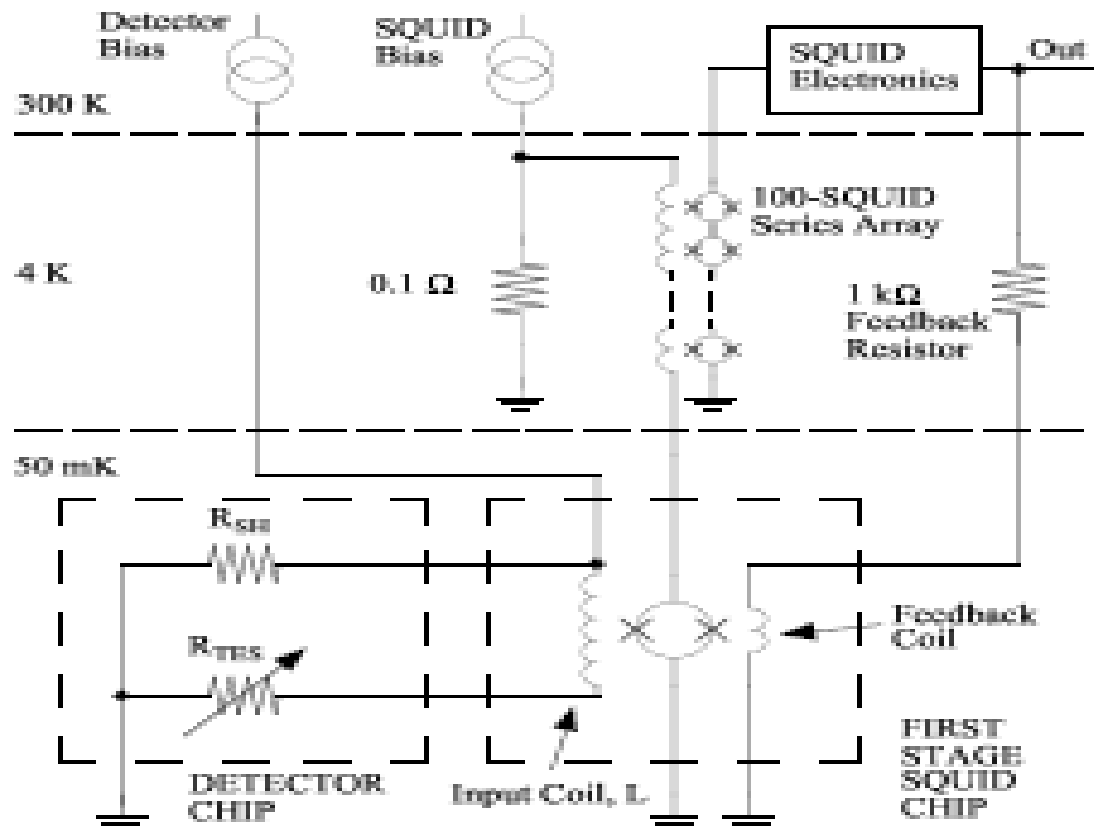
$$P = AK(T_2^n - T_1^n)$$

$$R(T) = R_0 \cdot \sqrt{R_s^2 + \left(1 - e^{-\frac{T_0 - T}{\tau}}\right)^2} \cdot H\left(1 - e^{-\frac{T_0 - T}{\tau}}\right)$$

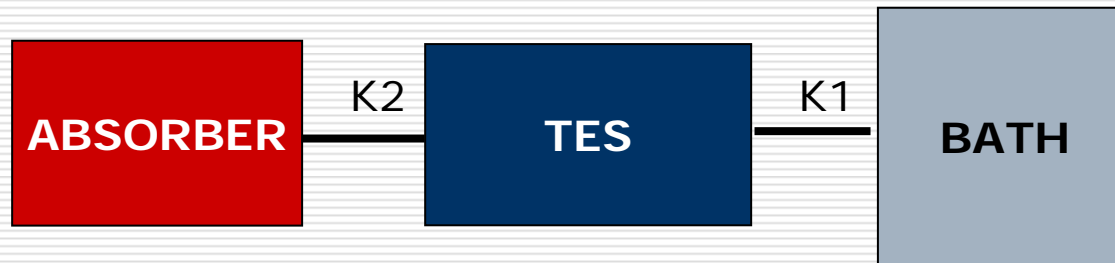
- $n=2,4,5$ (metal, dielectric or boundary, electron-phonon)

An example: insert the electronic parameters (case of SQUID amplifier)

- Make the electrical model of the readout circuit: example of SQUID readout of voltage biased microcalorimeter



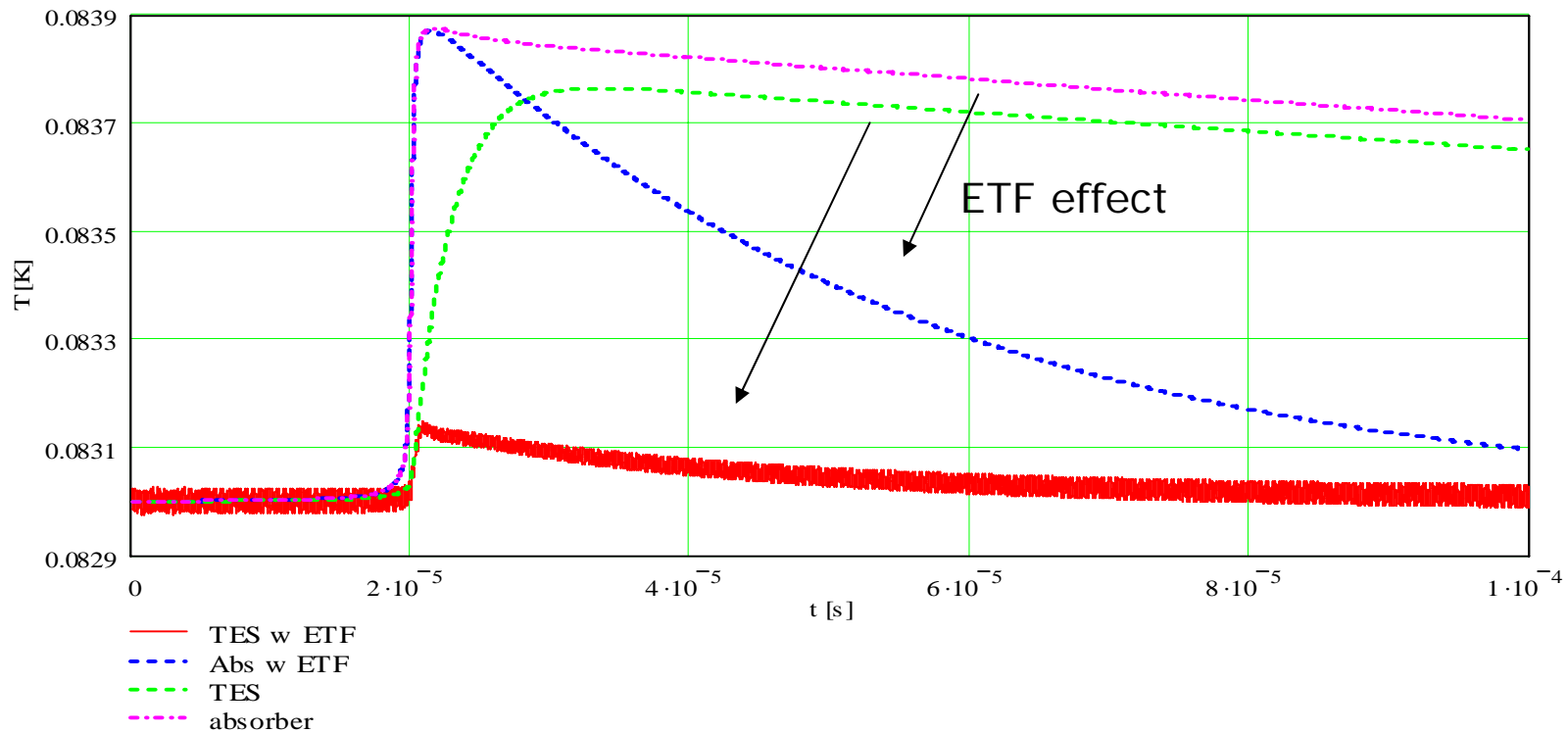
Build the minimal model: set of non linear equation → numerical solution is required



$$\left\{ \begin{array}{l} C_{TES} \frac{dT_{TES}}{dt} = K_2 (T_{Abs}^n - T_{TES}^n) - K_1 (T_{TES}^n - T_h^n) + R_x (T_{TES}) I_b^2 \\ C_{Abs} \frac{dT_{Abs}}{dt} = -K_2 (T_{Abs}^n - T_{TES}^n) + P_\beta (t) \\ R_{st} (I_0(t) - I_b) = R_x (T_{TES}) I_b + L_p \frac{dI_b}{dt} + \frac{q}{C} \\ I_b = \frac{dq}{dt} \end{array} \right.$$

Results: ETF clearly visible

- ETF: the bias power act as negative feedback reducing thermal swing and time response.
- ETF: Linearize and speed-up the response
- ETF: becomes important if L ranges is $\sim 10^{-1}$ - 10^2

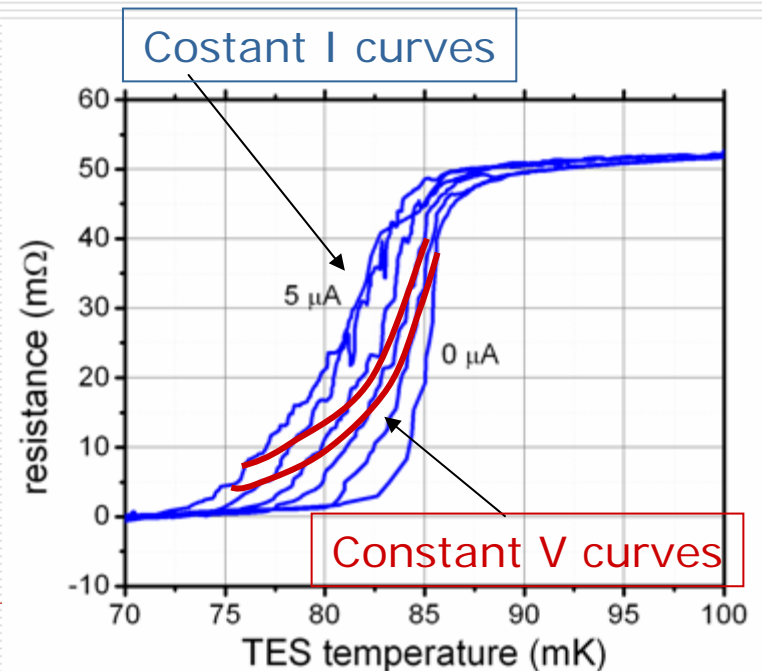
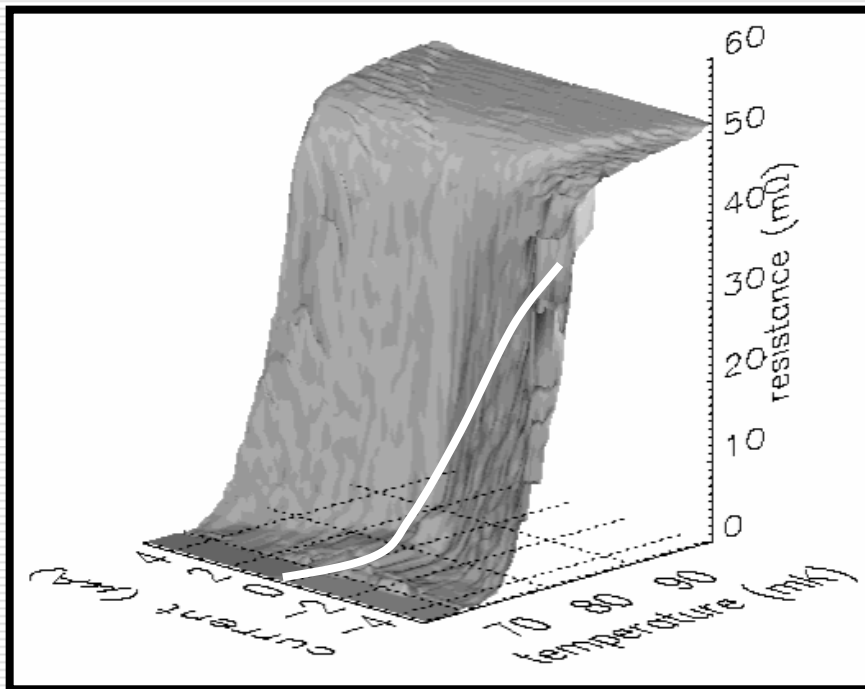


TES-Transition edge sensor

- Real TES sensor have T and I dependence

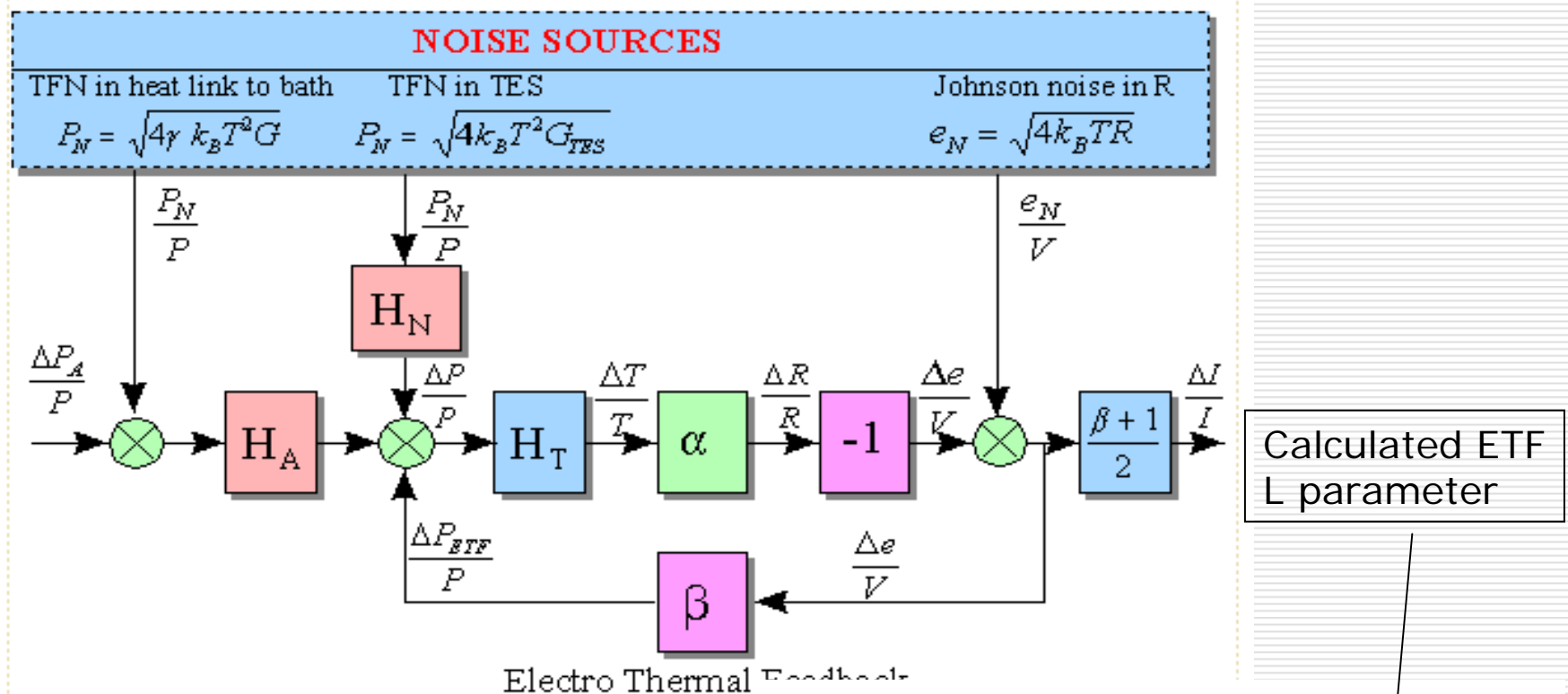
$$R(T, I) \approx R_0 + \left. \frac{dR}{dT} \right|_I \delta T + \left. \frac{dR}{dI} \right|_T \delta I \quad R(T, I) \approx R_0 + \alpha \frac{T}{R} \delta T + \beta \frac{T}{R} \delta I$$

- Dynamical performance much more complex to be evaluated



Whole model for the energy resolution for TES

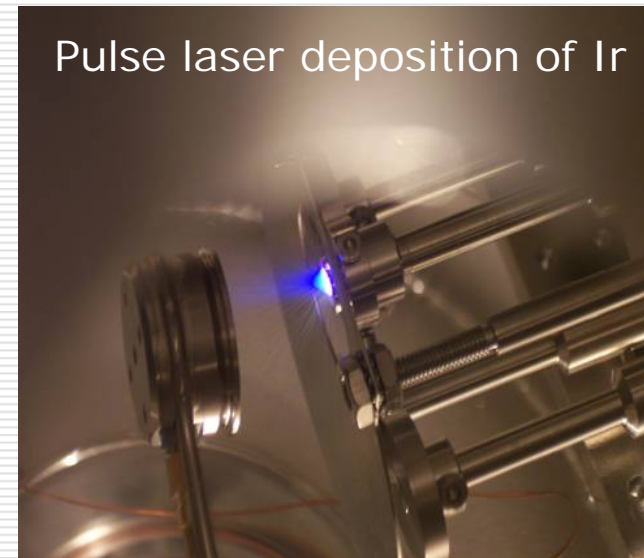
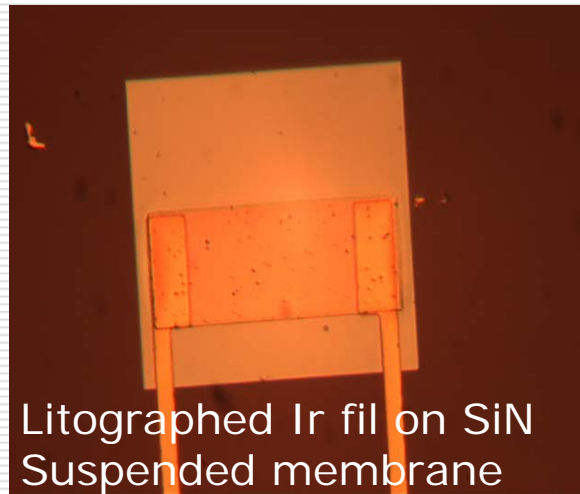
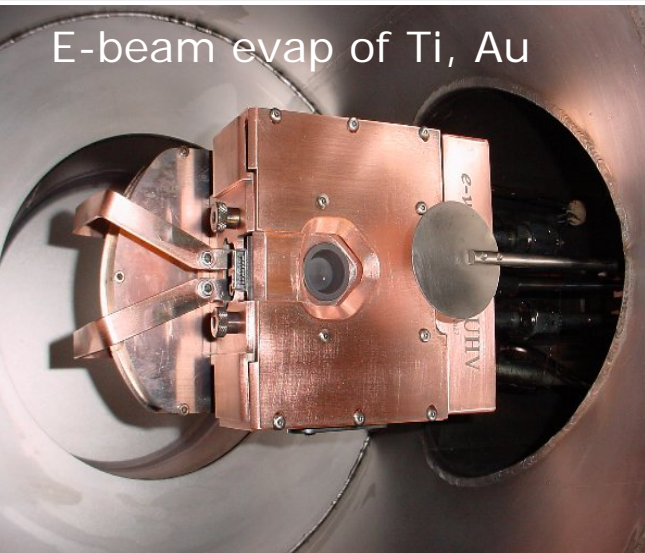
- Including all the noise sources (Phonon, Johnson...), the intrinsic thermal resolution contains sensor and conductance parameters: α and n ($\rightarrow G \sim T^n$)



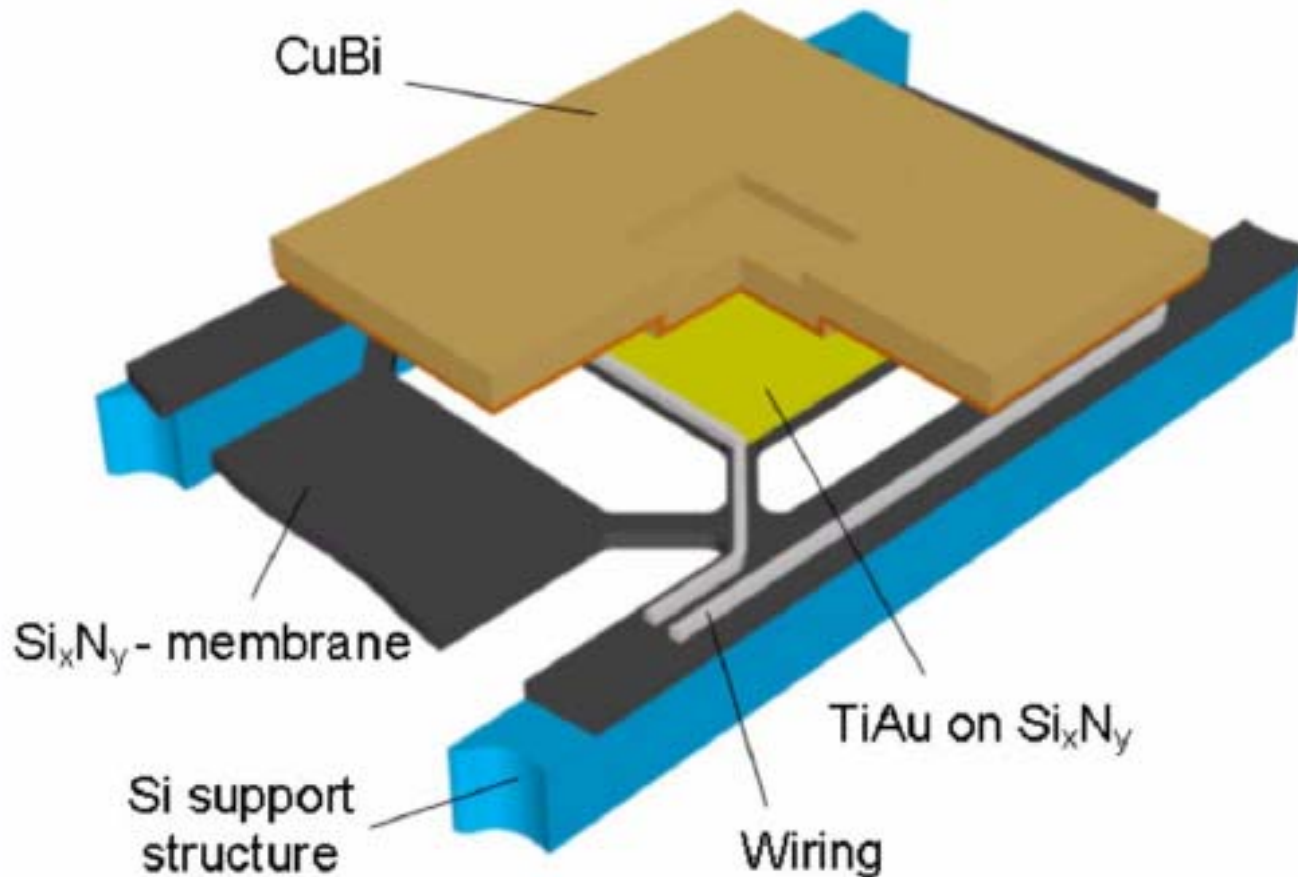
$$\delta E_{FWHM} = 2\sqrt{2 \ln 2} \sqrt{4k_B T_0^2 \frac{C}{\alpha_I} \sqrt{n/2}},$$

How TES are made of?

- They must have T_c in the 0.05-0.1 K range.
- Use of proximized Superconductors with metals: MoCu, TiAu, IrAu
- Film growth under high vacuum
- Lithography for all planar thin film process



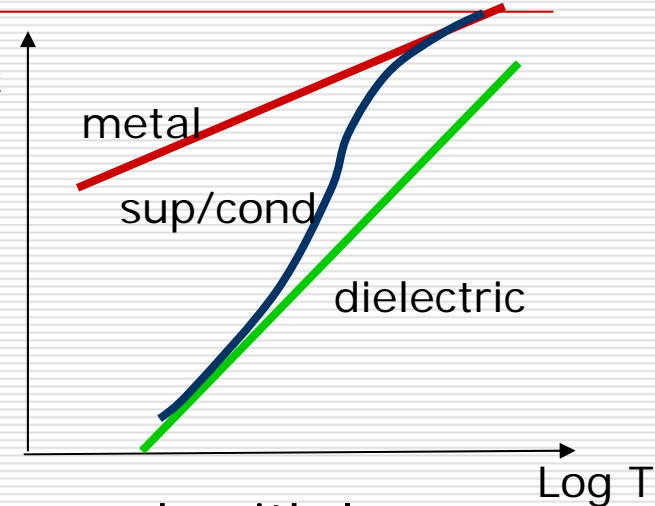
Present detector concept



Courtesy
SRON

Why absorbers are made with metals?

- Dielectric have lowest specific heat $\text{Log } C$
- Metals order of magnitude higher.
- Superconductor in the middle



- But, dielectrics or semiconductors produce e-h with long life, trapping the primary energy with time scale longer than the microcalorimeter time constant.
- Energy fluctuations are dominated by the well know e-h statistics: $(EFw)^{1/2} \gg (kT^2C)$
- Metals and Superconductors are the best choice for the ultimate performances: metals are faster then superconductors

Trapping effect in semiconducting Ge-NTD observed since the beginnings (D. McCammon et al, 1985) and further assessed in other works

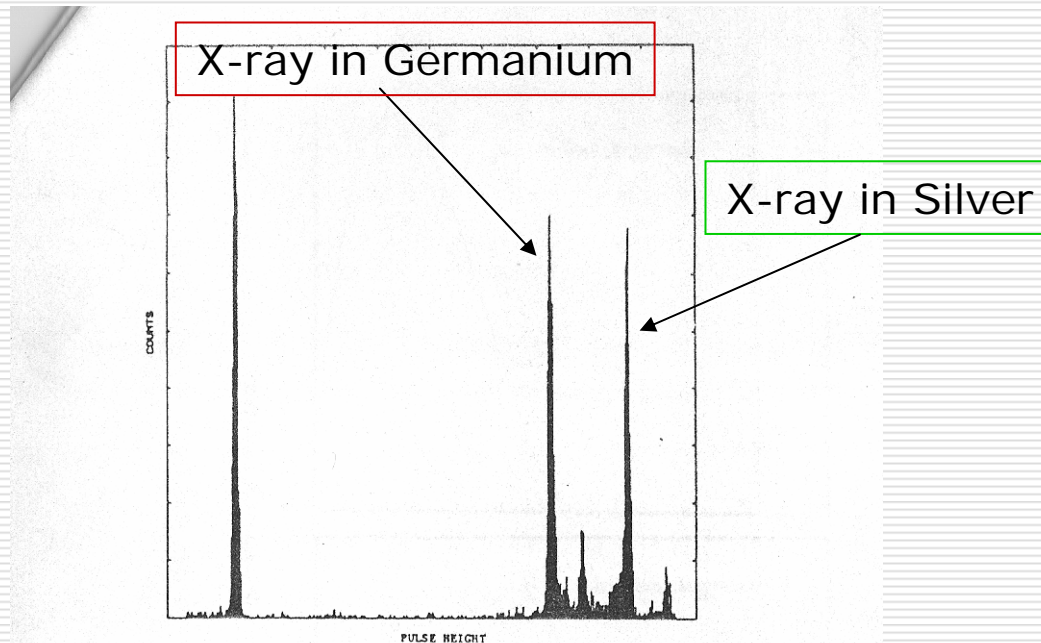
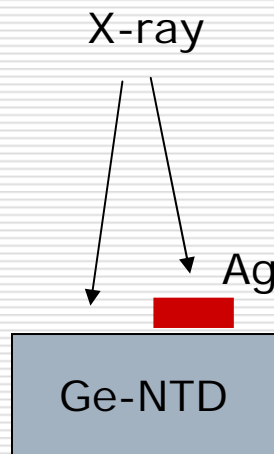
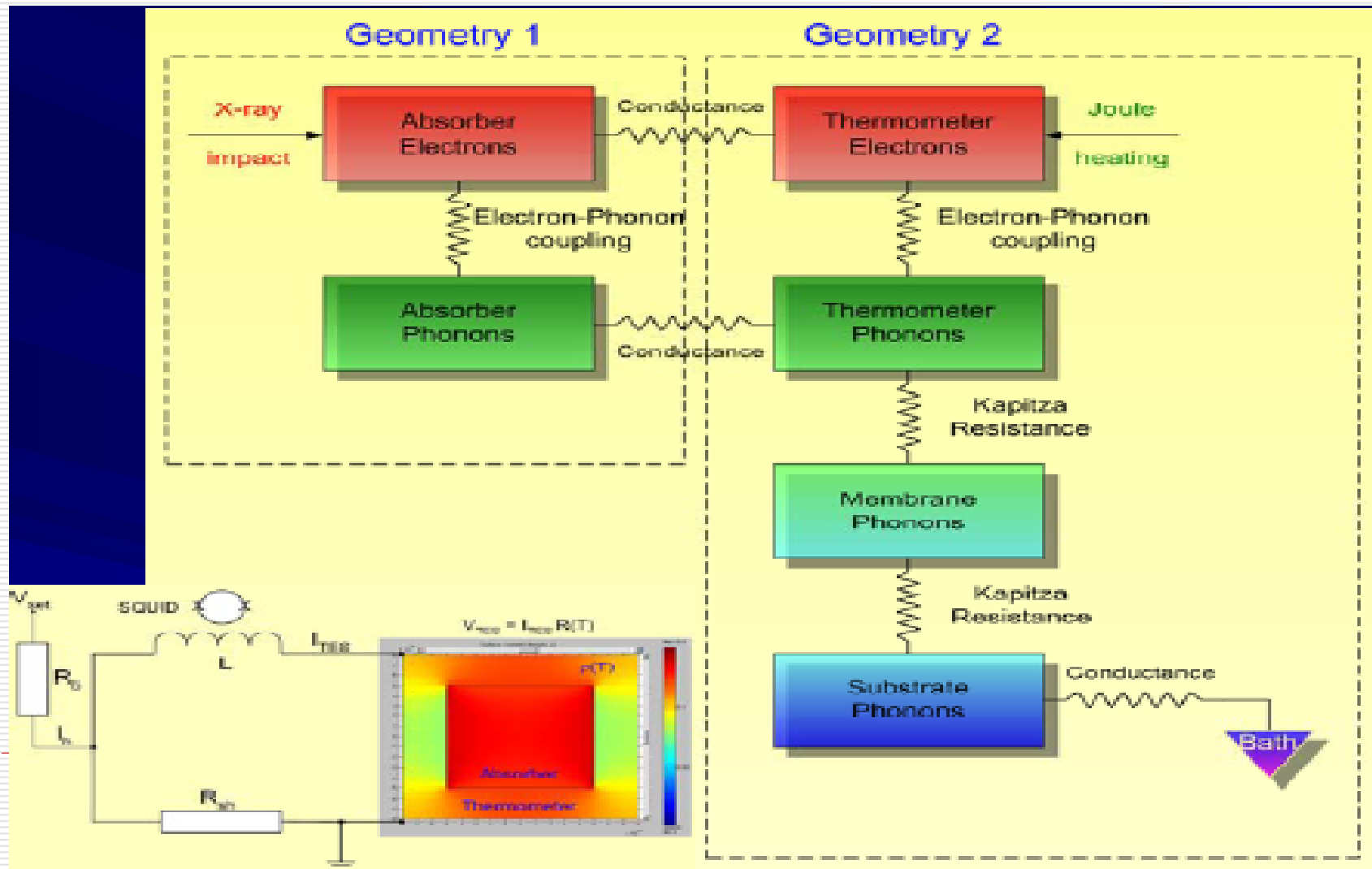


Fig. 4. Pulse height distribution of X-rays absorbed in a small dot of silver epoxy on the side of the germanium thermistor. The lower pair of peaks is due to X-rays which miss the epoxy and are absorbed directly in the germanium. *the single peak at the left*

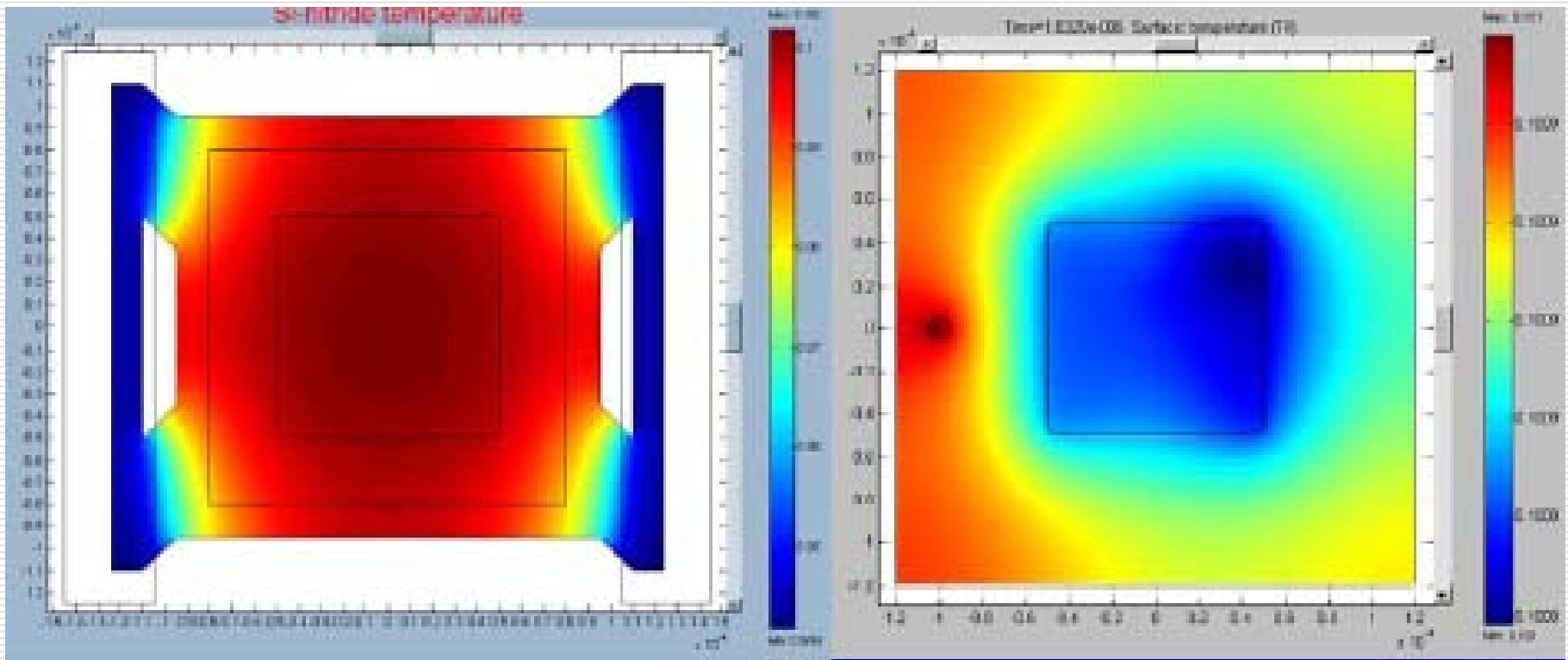
Thermal and electrical model



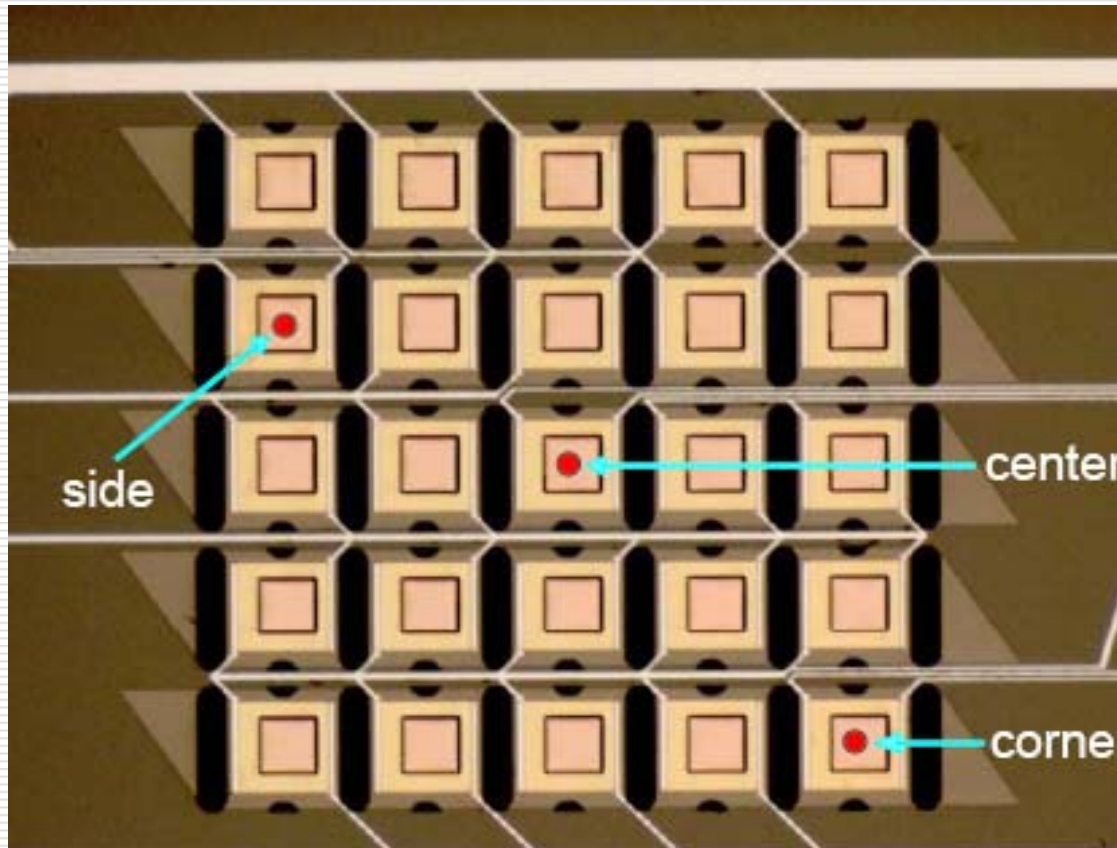
Why use of suspended Membranes?

→ Thermal model of SiN membrane and Absorber

- G can be tailored with micromachining
- All planar processes suitable for large integration



Array development by SRON



Single Pixel Performance (SRON)

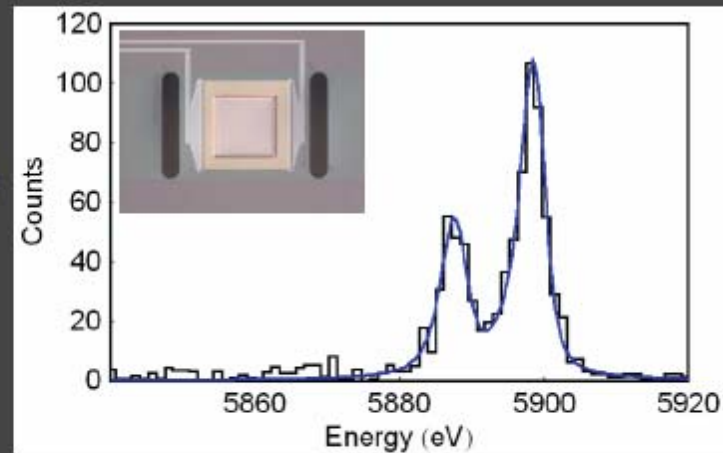
X-ray performance

Low heat capacity device

$$T_c = 105 \text{ mK}, E_{\text{sat}} = 5.5 \text{ keV}$$

$$\Delta E = 1.5 \text{ eV} \quad (320 \text{ eV, BESSY)}$$

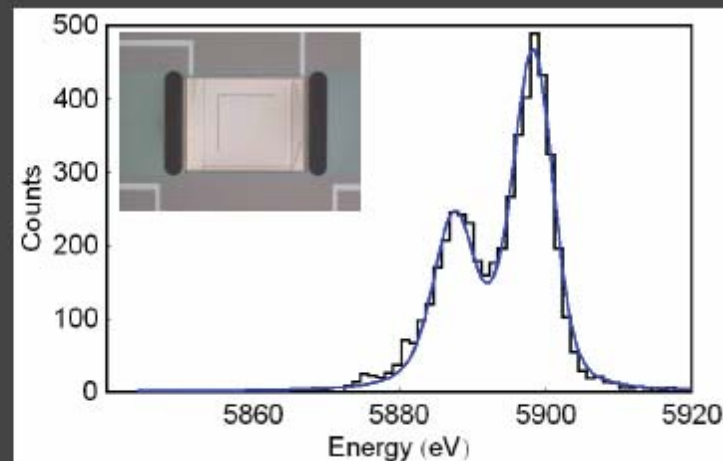
$$\Delta E = 2.5 \text{ eV} \quad (5.9 \text{ keV})$$



High heat capacity devices

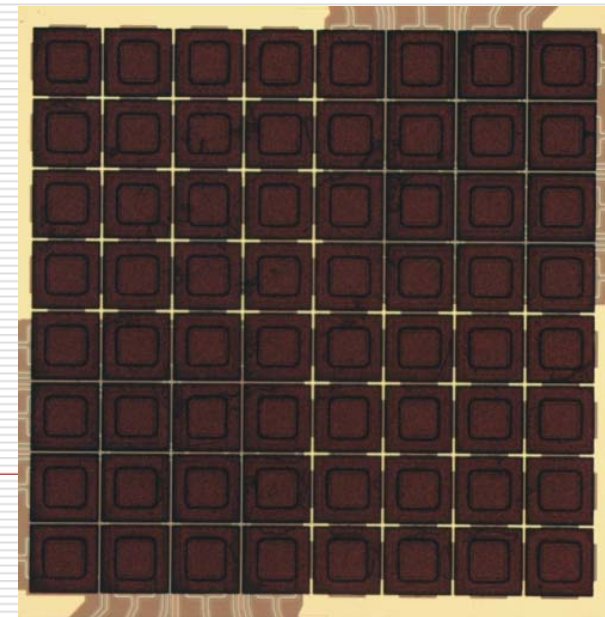
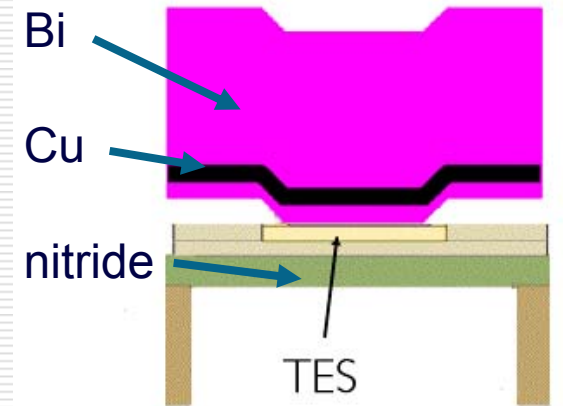
$$T_c = 125 \text{ mK}, E_{\text{sat}} = 17.3 \text{ keV}$$

$$\Delta E = 5.0 \text{ eV} \quad (5.9 \text{ keV})$$



NASA-Goddard developments

- Mo/Au TES
 - Electron-beam deposited
 - $T_c \sim 0.1$ K
 - Noise-mitigating normal-metal stripes
- Absorbers joined to TES in micro-fabrication
 - “Mushroom” shaped to cover the gaps
- Emphasis on absorbers needed for Constellation-X reference design
 - 0.25 mm pitch (TES is 0.13 mm wide)
 - 92% fill factor
 - 95% QE at 6 keV



NASA-Goddard developments

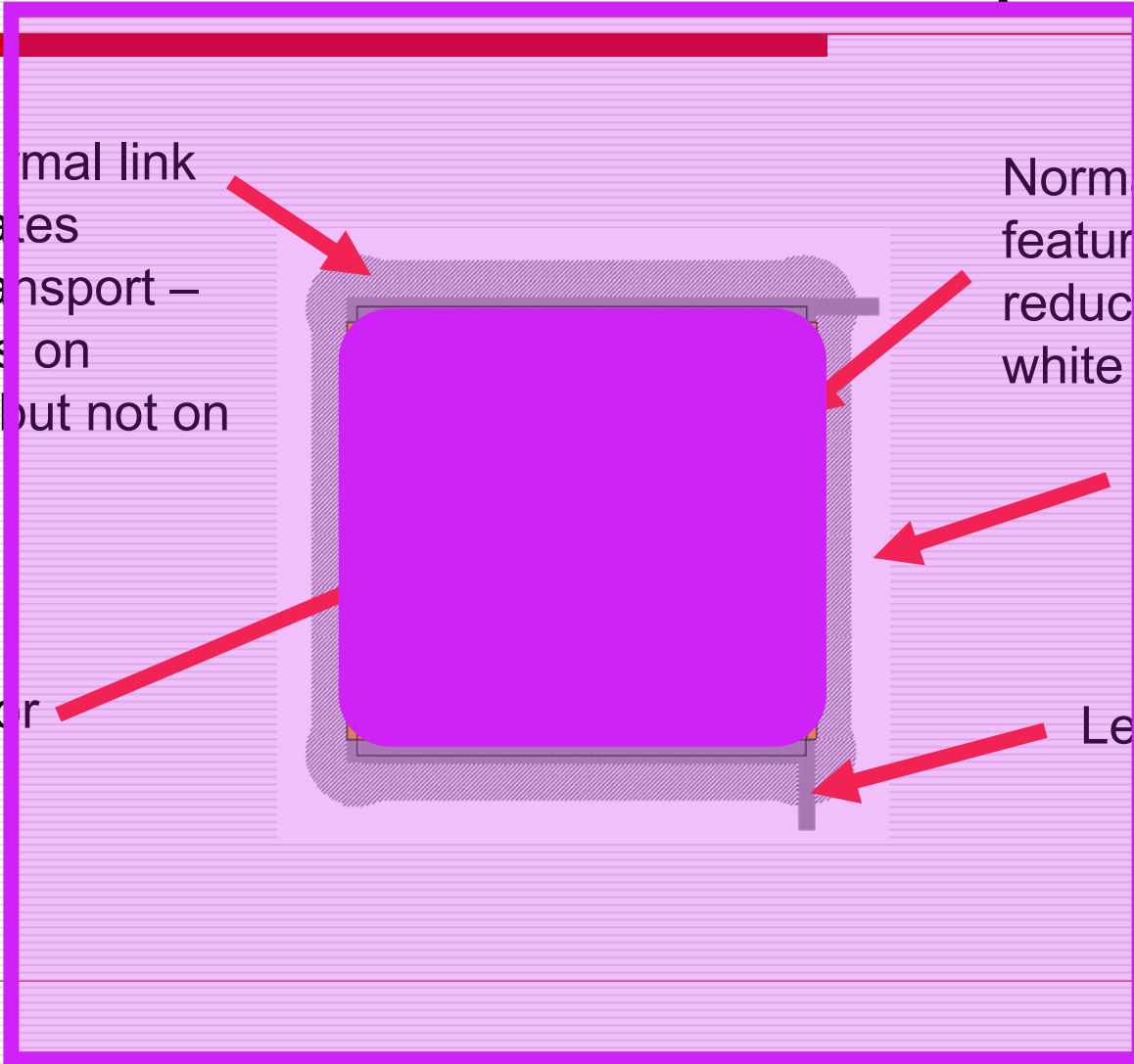
Nitride thermal link demonstrates ballistic transport – G depends on perimeter but not on extent

Normal metal features to reduce excess white noise

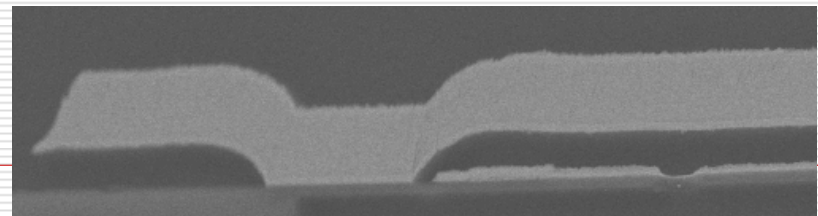
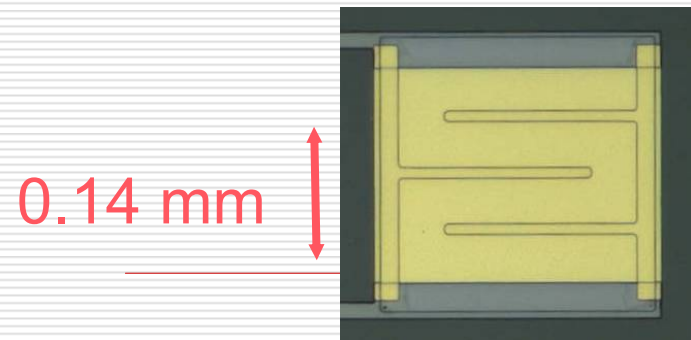
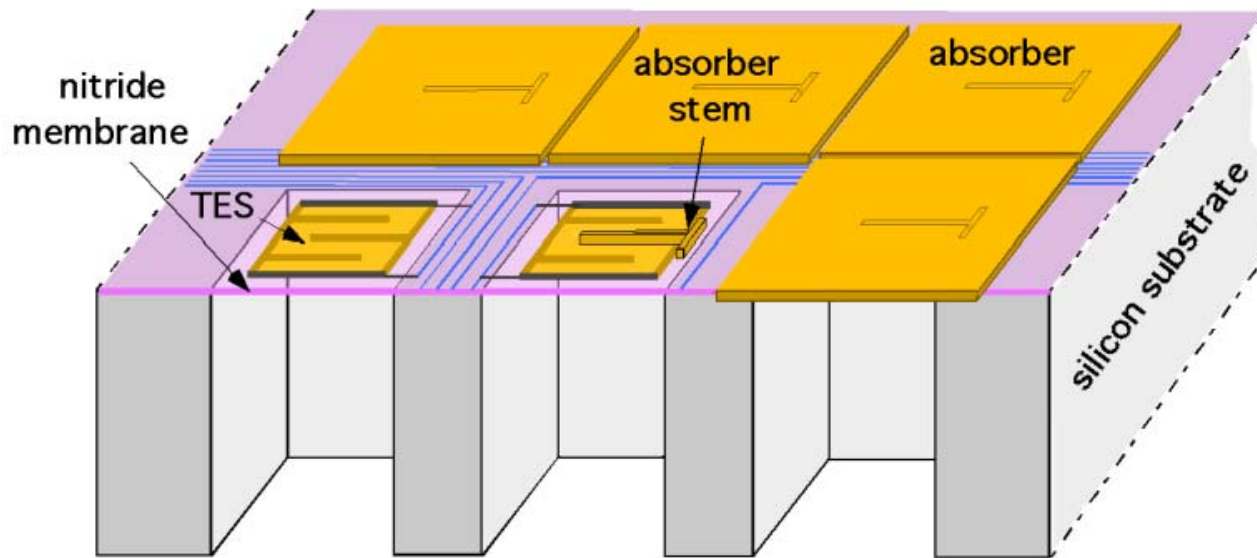
Silicon at 55 mK

Sensor

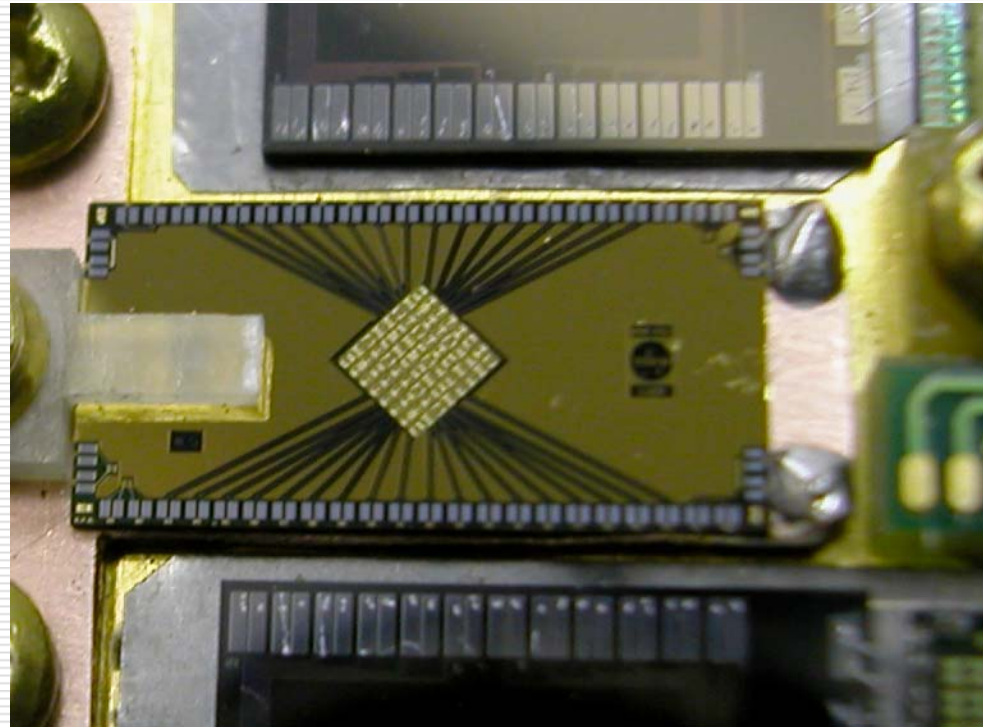
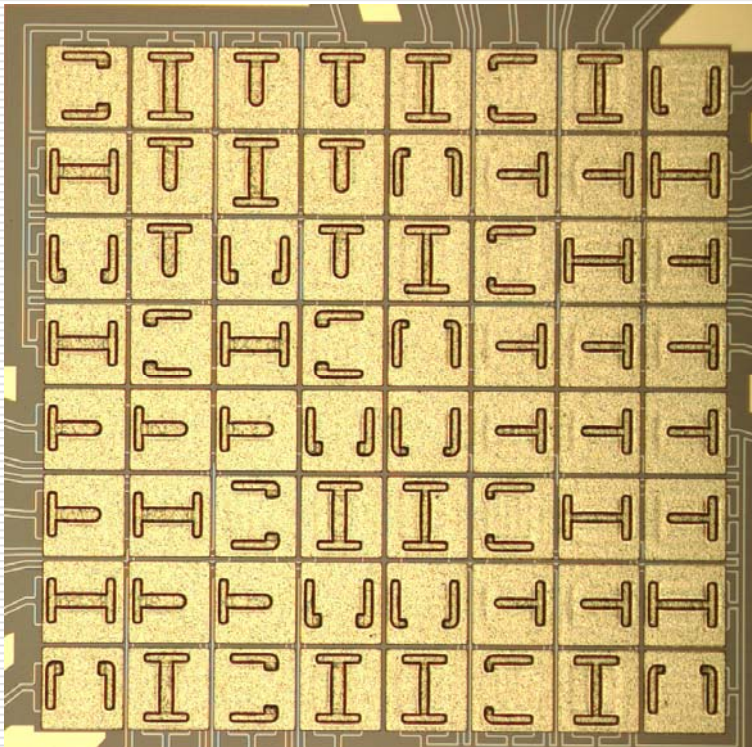
Leads



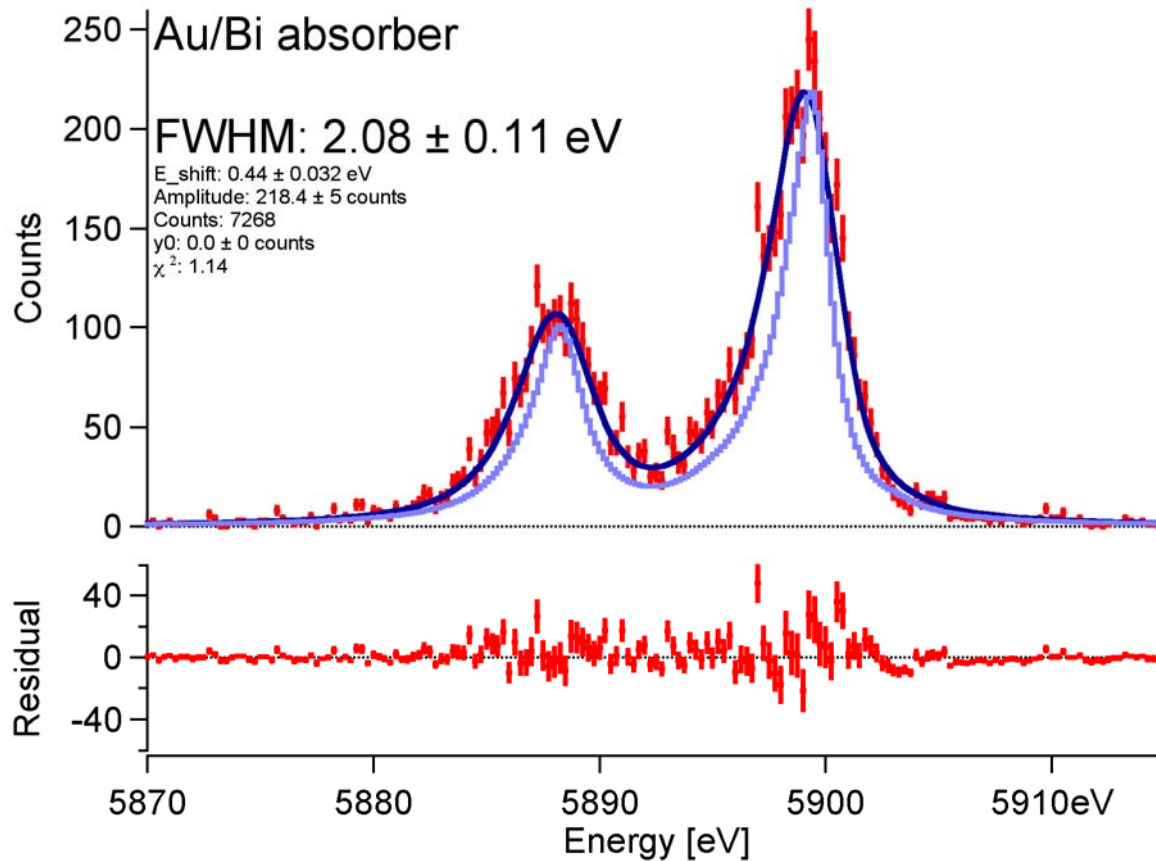
New method for absorber fabrication (Gold)



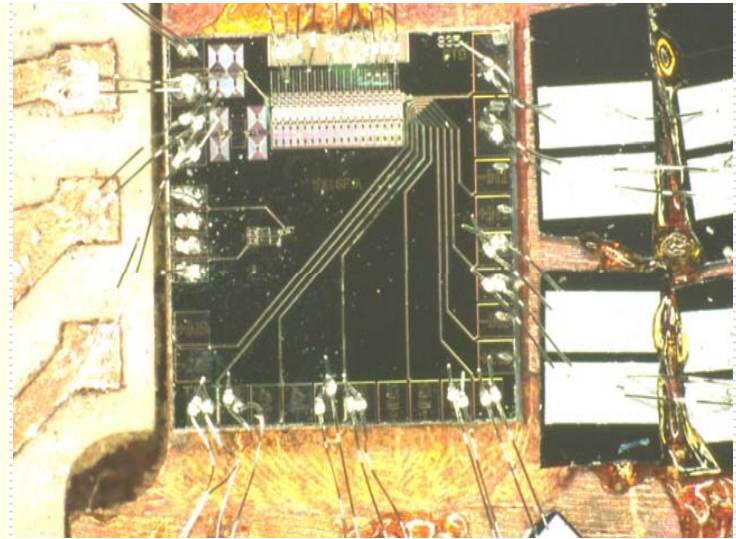
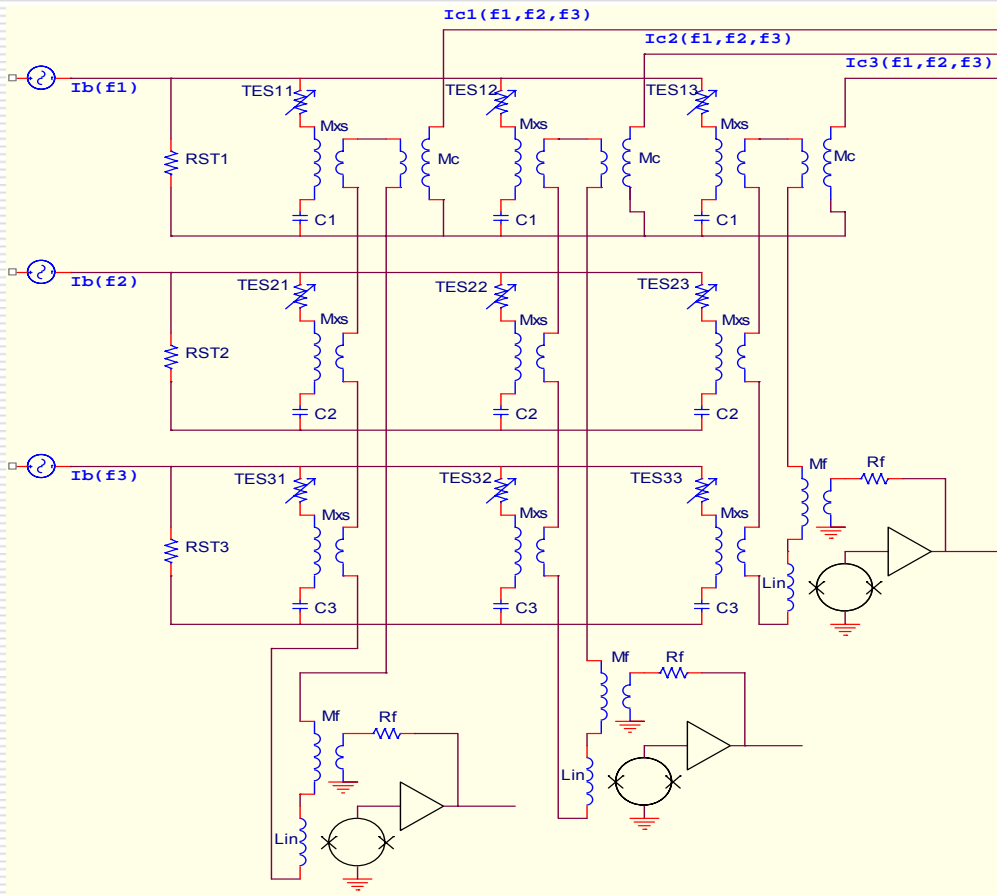
NASA-Goddard developments



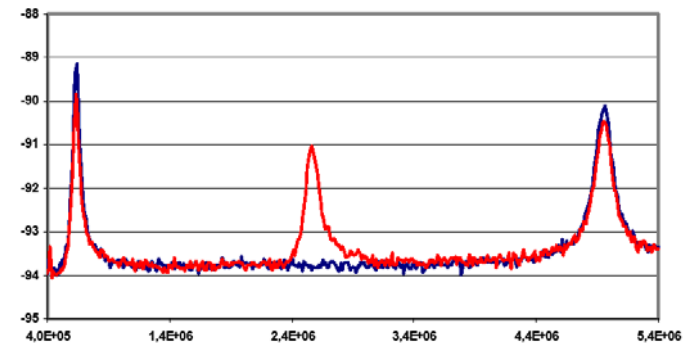
NASA-Goddard developments



Electronics: needed MUX readout. Many developments. An example: development of TDM MUX readout in Italy



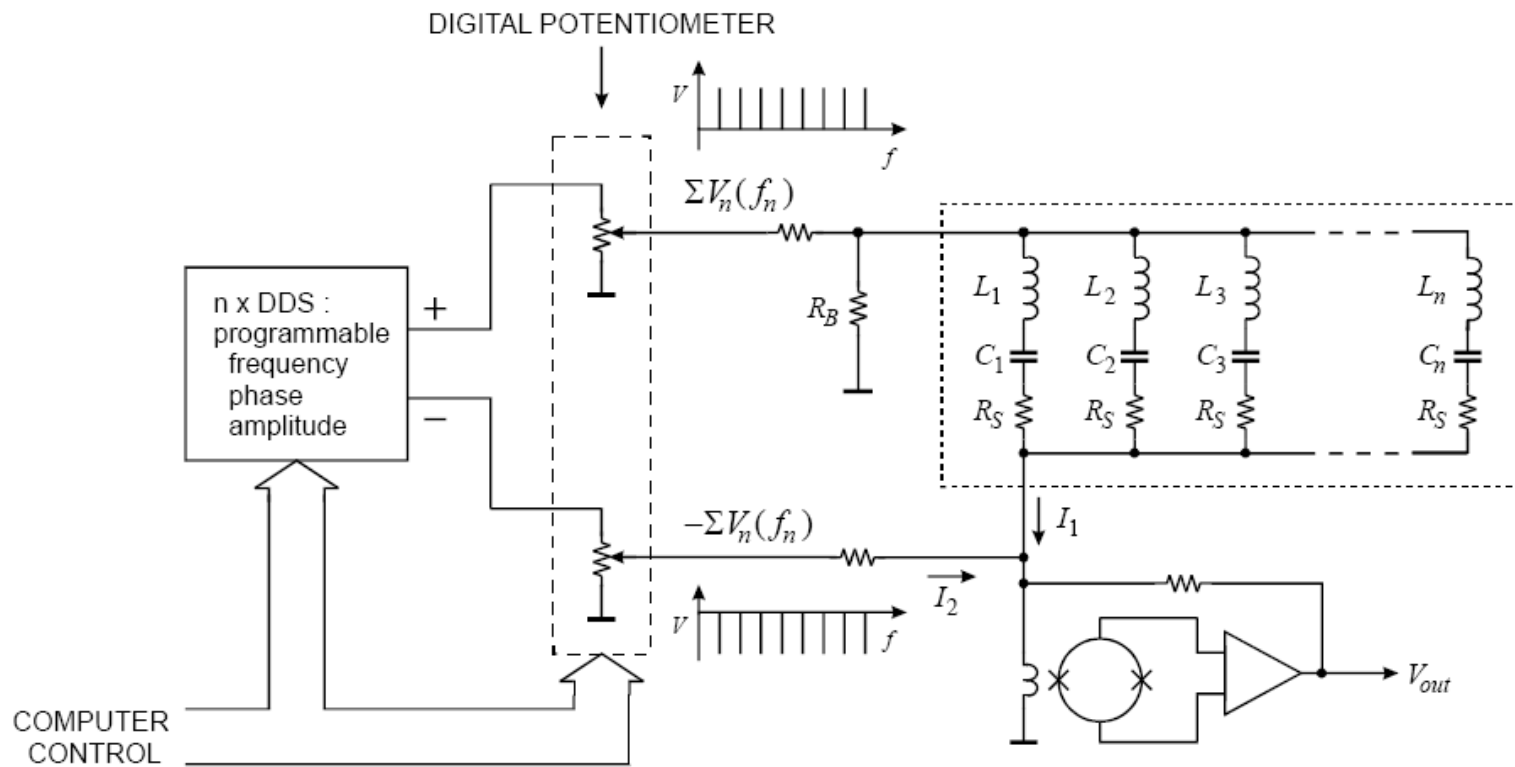
Red = 25 mK
Blue = 112 mK



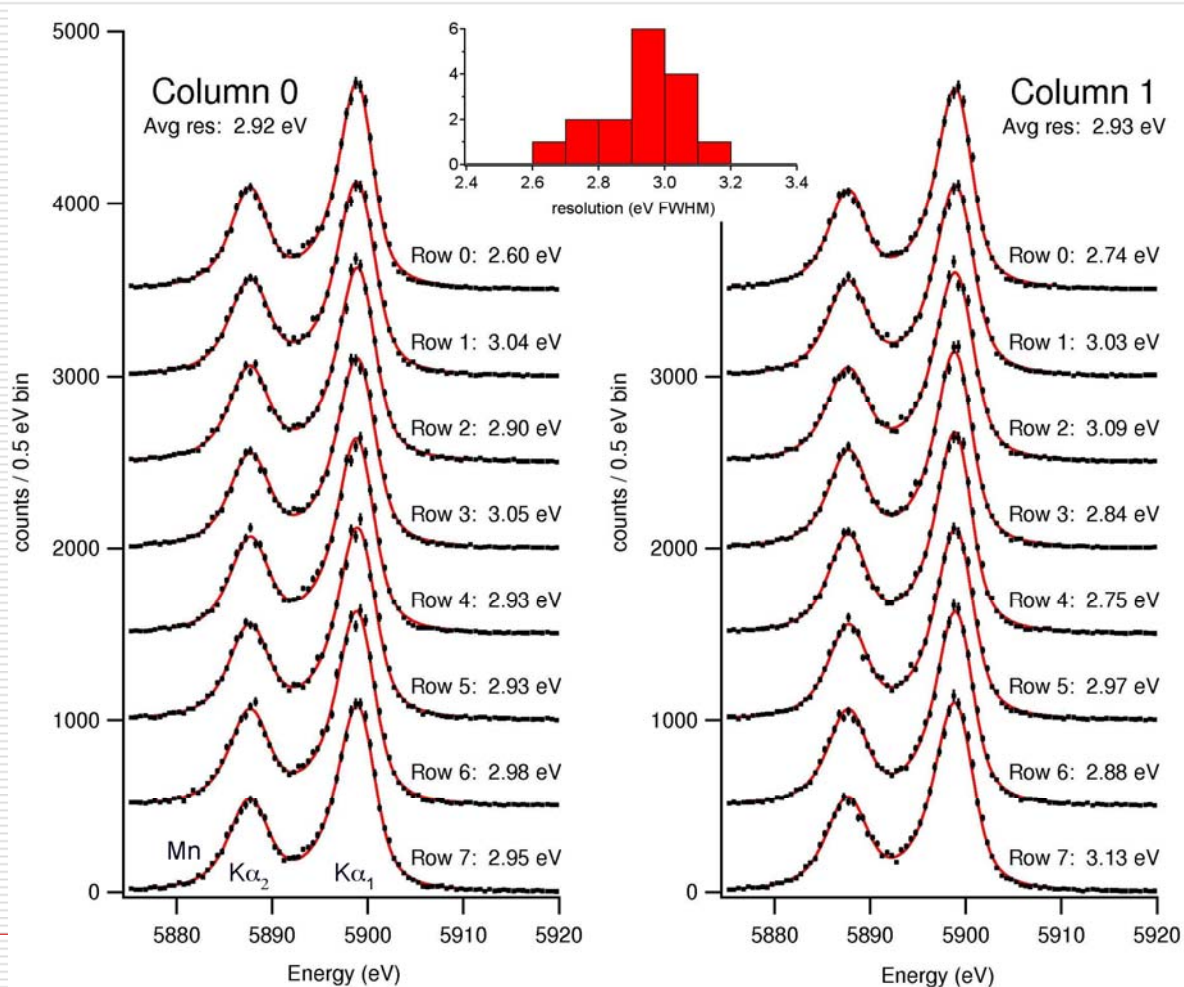
TES detectors could be a flight instrument for a next X-ray missions

- ❑ Huge effort in US, EU, Japan
 - ❑ US projects led mainly by GSFC → 2 eV fwhm, mux readout of 2x8 pixels (Con-X, NEXT)
 - ❑ EU projects (+ Japan) in EURECA consortium led by SRON: 2.5 eV fwhm, mux readout in final assessment phase, 5 eV high C detector. Same performance (4.6 eV) obtained by our the Italian group with high C microcal (XEUS, EDGE).
 - ❑ Japan: single pixel at 4.5 eV, fast development of detector/electronics (NEXT)
-

Multiplexed Readout (principles)

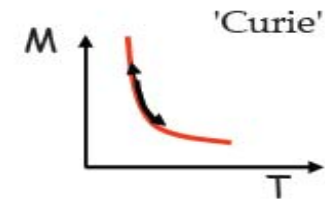
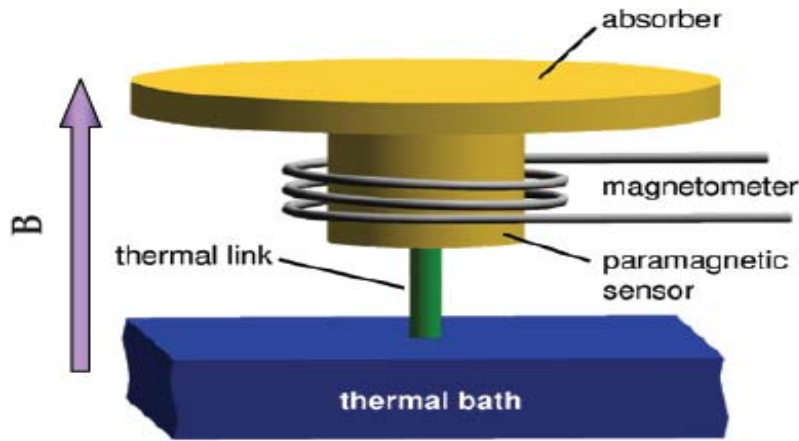


From the present 2x8 , to 32x32 pixel array as next goal of GSFC



Magnetic Microcalorimeter: a possible new promising technology (Heidelberg group)

Metallic magnetic calorimeters



$$\delta M = \frac{\partial M}{\partial T} \delta T = \frac{\partial M}{\partial T} \frac{E}{C_{tot}}$$

Very simple theory :

Sensor material consists of magnetic moments only

2 level systems

Zeeman like energy splitting $\Delta E = m \cdot B$

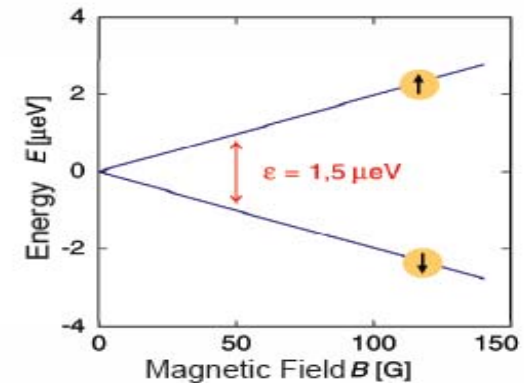
$\epsilon \approx 1.5 \mu\text{eV}$

Energy deposition of 100 keV

Number of flips $\approx 10^{11}$

Change of magnetic moment

$$\Delta m = \frac{\Delta E}{B} \approx 10^{11} \mu_B$$



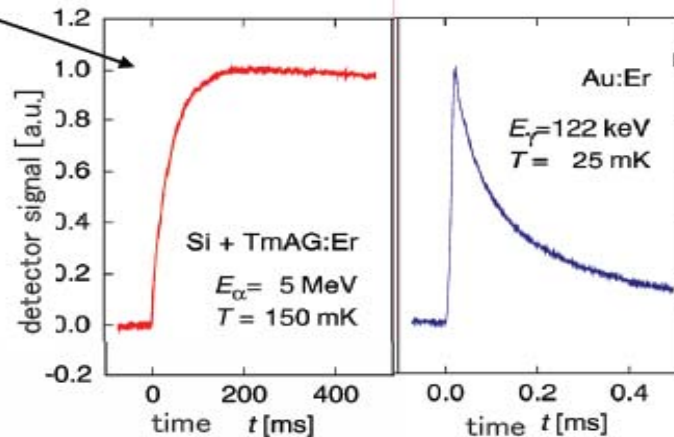
Heidelberg developments

Response times of magnetic calorimeters

Dielectric paramagnets :
(Bühler & Umlauf '93)



$\tau \approx 50 \text{ ms}$



Paramagnetic alloys (e.g. Au:Er):
(Heidelberg & Brown Univ.)



$\tau < 1 \mu\text{s}$

$\gg 100 \text{ counts/s}$ possible

response time of electronics:
presently 1-10 μs

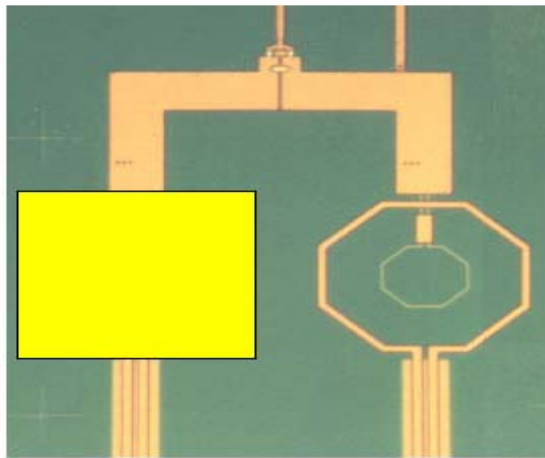
Sensor material presently used \rightarrow

Au:Er with Erbium concentration of few hundred ppm

Heidelberg developments

Magnetic calorimeter for x-ray spectroscopy

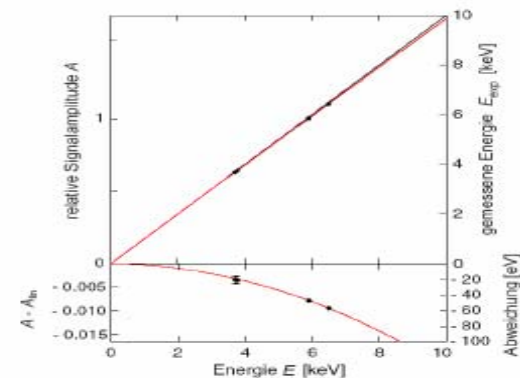
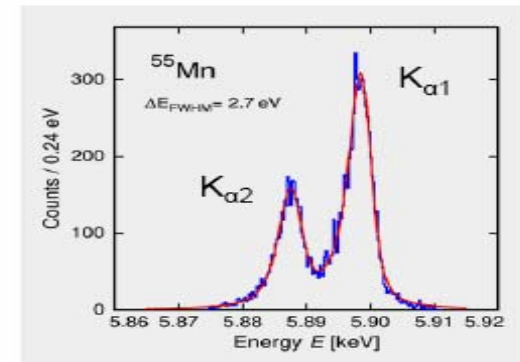
Characterization with ^{55}Fe -Source:



energy resolution $\Delta E_{\text{FWHM}} = 2.7 \text{ eV}$

resolving power 2200

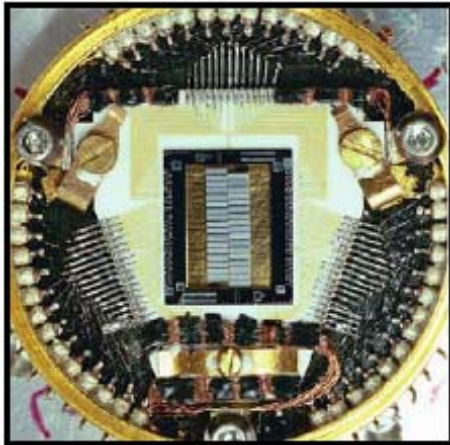
non-linearity at 6keV: $< 0.8\%$



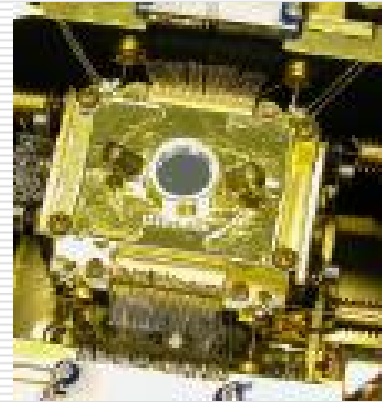
Conclusions

- ❑ TES microcalorimeters have achieved the goal performance in High Spectral Resolution (2 eV fwhm @ 6KeV) for application to the next missions (ConX-XEUS)
 - ❑ Further improvements are under way mainly for increasing the array size.
 - ❑ Other promising techniques are under study: magnetic calorimeters, KID sensors
 - ❑ Advancement in readout techniques and refrigeration technology will allow fall-outs in many other fields (material science, security, pollution monitoring,...)
-

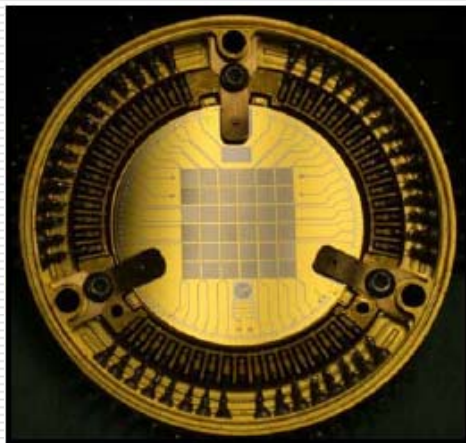
Don't forget the first array with Si doped sensors for XQC and ASTRO-E that have operated in sounding rockets and in orbit



XQC for sounding
rocket
Old detector



XRS on AstroE



XQC for sounding
rocket
New detector



XRS operated
Few weeks before
the cryo failure
